MODELING CONTROL OF HIV INFECTION THROUGH STRUCTURED TREATMENT INTERRUPTIONS WITH RECOMMENDATIONS FOR EXPERIMENTAL PROTOCOL

Shannon Kubiak[1], Heather Lehr[2], Rachel Levy[3], Todd Moeller[4], Albert Parker[5], Edward Swim[6]

Problem Presenter:
Sarah Holte, Ph.D.
Fred Hutchinson Cancer Research Center
Seattle, WA 98109

Abstract

Highly Active Anti-Retroviral Therapy (HAART) of HIV infection has significantly reduced morbidity and mortality in developed countries. However, since these treatments can cause side effects and require strict adherence to treatment protocol, questions about whether or not treatment can be interrupted or discontinued with control of infection maintained by the host immune system remain to be answered. We present sensitivity analysis of a compartmental model for HIV infection that allows for treatment interruptions, including the sensitivity of the compartments themselves to our parameters as well as the sensitivity of the cost function used in parameter estimation. Recommendations are made about collecting data in order to best estimate the most sensitive parameters in the model. Furthermore, we present parameter estimates using simulated data.

1 Introduction

Highly Active Anti-Retroviral Therapy (HAART) has been highly successful in reducing the viral load in HIV patients. However, the combined expense and side effects of this therapy have had a negative impact on drug distribution and patient compliance. Studies indicate [1], [2] that Structured Treatment Interruptions (STI) which involve periods of time during which patients receive no medication, may actually be beneficial to the patient. These interruptions stimulate the immune system and potentially induce a state in which the immune system controls the viral infection.

In this workshop, we examined a modified version of the Wodarz-Nowak model for HIV infection dynamics. As a step toward finding a treatment protocol involving STI that will induce host control of the virus, we performed a sensitivity analysis of our model. This sensitivity analysis suggests future experimental design to test the model and theory of STI for control of HIV. Our investigation sought the most sensitive parameters and compartments as well as the optimal time schedule for data collection. We also considered the parameter identification problem that would use data to estimate parameters in the model.

In Chapter 2, we will describe the modifications made to the Wodarz-Nowak model and the effects those changes make to the dynamics of the problem. In Chapter 3 we describe the sensitivity analysis that was conducted and the resulting recommendations for experimental protocol. Finally, in Chapter 4 we present the parameter estimation results we computed using simulated data.

2 Description of the Modified Wodarz-Nowak Model

The goal of this workshop was to examine a modified version of the Wodarz-Nowak model [3] for HIV infection dynamics. The modification involves the addition of an extra compartment, V, to represent the viral load present. The change in viral load over time is modeled as a difference of a linear birth rate dependent on the number of infected cells and a death rate of the short-lived virus.

[1]Towson University
[2]University of Texas at Austin
[3]North Carolina State University
[4]Georgia Institute of Technology
[5]Montana State University - Bozeman
[6]Texas Tech University

2.1 ODE Model

The model is a coupled system of five ordinary differential equations with twelve parameters. Here the state variables describe compartments in the biological system. Our modification of the Wodarz-Nowak Model for HIV infection dynamics is

$$\begin{aligned}
\dot{X} &= \lambda - d\,X - \beta\,[1 - f\,u(t)]\,XV \\
\dot{Y} &= \beta\,[1 - f\,u(t)]\,XV - a\,Y - p\,YZ \\
\dot{W} &= c\,XYW - cq\,YW - bW \\
\dot{Z} &= cq\,YW - h\,Z \\
\dot{V} &= k\,Y - \mu\,V,
\end{aligned}$$

where the compartments are

$$\begin{aligned}
X &= \text{Uninfected T helper cells} \\
Y &= \text{Infected T helper cells} \\
W &= \text{Immune Precursors Cytotoxic T Lymphocyte} \\
Z &= \text{Immune Effector Cytotoxic T Lymphocyte} \\
V &= \text{Free Virus},
\end{aligned}$$

and the parameters are

$$\begin{aligned}
\lambda &= \text{Target cell production rate} \\
d &= \text{Natural death rate of target cells} \\
\beta &= \text{Rate of viral replication} \\
f &= \text{Treatment efficacy factor} \\
a &= \text{Natural death rate of Infected cells} \\
p &= \text{Death rate of infected cells due to immune response} \\
c &= \text{CTL activation rate} \\
q &= \text{Growth rate of CTL effectors due to infected cells and CTL precursors} \\
b &= \text{Natural death rate of CTL precursors} \\
h &= \text{Natural death rate of CTL effectors} \\
k &= \text{Growth rate of virions due to infected cells} \\
\mu &= \text{Natural death rate of virions.}
\end{aligned}$$

In the model, we assume the virus instantaneously approaches T-cells with no time lag for diffusion. It is important to note that such a delay probably exists, but is not modeled by our system. Also note that the compartment V only represents virions that can infect uninfected cells (represented by the X compartment). In this model, immune precursors (W) are stimulated by infected cells, not by the virus. Figure 1 visually represents the relationship between the compartments in the modified Wodarz-Nowak Model.

2.2 Incorporation of Structured Treatment Interruption (STI) in the Model

Structured treatment interruptions are planned times that patients will cease taking medication. In this model, it is assumed that STI is incorporated only after the patient has been on medication long enough to maintain a low level of viral load. Then, during a treatment interruption, the virus level rises and consequently stimulates the immune system. The refreshed immune system may (hopefully!) then suppress the viral load without the aid of continued medication.

The function $u(t)$ represents the incorporation of STI in our model. Values of $u(t)$ range from 0 to 1, with 0 representing no treatment and 1 representing full treatment. Thus $u(t)$ effectively reduces the infectivity

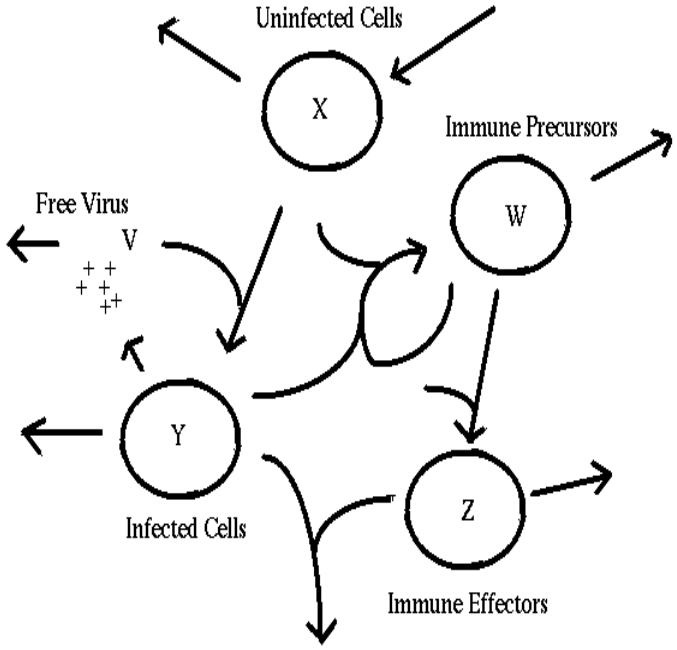

Figure 1: Relationship between compartments in the modified Wodarz-Nowak model. Uninfected T-helper cells X are infected by free virus V to become infected T-helper cells Y. The infected cells stimulate the immune precursors W to become immune effectors Z that can in turn kill the infected cells. The model includes other relationships, but these are the primary interactions between compartments in the model.

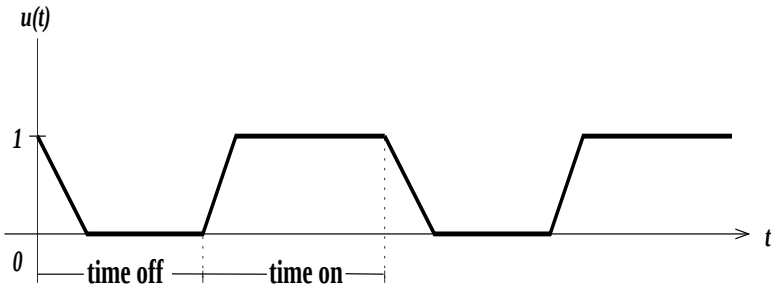

Figure 2: The function u(t) which incorporates STI in the model. Our work assumes a drug rise time of two days and decay time of four days.

parameter (β) of the system as it grows from 0 to 1. In our analysis we considered a periodic STI schedule, $u(t)$, of the form shown in Figure 2.

The parameter f represents the efficacy of the treatment, for which we assumed a value of 0.75. It is important to note that independent investigations by Brian Adams (a graduate student advising our group) suggest that the behavior of the model is radically different for $f < 0.95$ than for $f > 0.95$.

2.3 Equilibria and Choice of Parameter Values

The parameters in our work are derived from those used by Wodarz and Nowak, whose model has a basic viral reproductive ratio, $R_0 = \beta\lambda/ad = 25$. As mentioned earlier, our model consists of their model together with a compartment for free virus. Adding this free virus compartment results in a basic viral reproductive ratio, $R_0 = \beta\lambda k/ad\mu$. To calculate parameters for our modified model, we made three assumptions:

1. the same basic viral reproductive ratio ($R_0 = 25$);
2. a ratio of our new parameters: $k/\mu = 25$, since accepted values for these parameters are $k \in [20, 250]$ and $\mu = 1$; and
3. $\beta k = 0.5$ for our new parameter set, where 0.5 is the value of β used by Wodarz and Nowak.

The last condition (3) is enforced because in our model, the dynamics for V depend largely on kY. Consequently the dynamics for Y, which include βXV, indirectly depend on βk. These assumptions yield the following parameters, which were used in our simulations.

Parameter	Value
λ	1
d	0.1
β	0.02
a	0.2
p	1
c	0.027
q	0.5
b	0.001
h	0.1
k	25
μ	1
f	0.75

This model has multiple equilibria for all parameter sets $\mathbf{q} = [\lambda, d, \beta, a, p, c, q, b, h, k, \mu, f]^T$, but the stability of each of these equilibria depends on the choice of parameters. For the choice of parameters used in the simulations ($\mathbf{q_0}$), there are two stable equilibria which correspond to the success or failure of the immune system to control infection. The equilibrium values corresponding to our parameters are given in the following table.

Compartment	1st Equilibrium (virus dominates)	2nd Equilibrium (immune system dominates)
X	0.4	9.8
Y	4.8	.004
W	0	8751
Z	0	4.7
V	120	0.10

Our stability analysis is localized at the point $\mathbf{q_0}$ in the parameter space. We linearize the non-linear system about an equilibrium point, then carry out an eigenvalue analysis. [4] This produces only local stability results. We would expect different numerical results if we localized our study at different parameter values. In solving the parameter identification problem, values for our parameter vector $\mathbf{q}$ were chosen from the set Q_{ad}, the space of valid values for $\mathbf{q}$.

3 Analysis

Because the modified Wodarz-Nowak model is complex, including five compartments and twelve parameters, it is necessary to establish priorities about which parameters to estimate and which compartments to try to observe. A sensitivity analysis informs this prioritization, which can aid in experimental design.

The sensitivity analysis has three goals. First, in order to choose a subset of parameters to estimate, it is necessary to determine which parameters to play a significant role in the dynamics of the model. Second, in order to suggest a timing schedule for collection in the experimental protocol, it is necessary to determine which times are most critical for data collection. Third, in order to determine which compartments are necessary to observe and whether or not their observation can be combined, it is necessary to determine which combinations of compartments play a significant role in the dynamics of the model.

3.1 Derivation of the Sensitivity Matrix

In this subsection, we find an equation for the sensitivity matrix, $\partial z/\partial q$, from our model. This will suggest the sensitivity of the states to the parameters. Recall that our model has five compartments, $\mathbf{z} = [X, Y, W, Z, V]$ and twelve parameters, $\mathbf{q} = [\lambda, d, \beta, a, p, c, q, b, h, k, \mu, f]$. We can therefore represent our model by

$$\dot{\mathbf{z}} = f(\mathbf{z}(t); \mathbf{q}),$$

$$\mathbf{z}(0) = \mathbf{z_0}.$$

Differentiating with respect to q and formally passing the time derivative through yields

$$\left(\frac{\dot{\partial z}}{\partial q}\right)(t) = \frac{\partial f}{\partial z}(z(t, q_0); q_0) \cdot \frac{\partial z}{\partial q} + \frac{\partial f}{\partial q}(z(t, q_0); q_0).$$

This can be written as an $n \times m$ matrix system ($n = 5, m = 12$) of ODEs for the sensitivity matrix $r(t) = \partial z/\partial q$

$$\dot{r}(t) = A_0(t)\, r(t) + g_0(t),$$

$$r(0) = 0,$$

where

$$A_0 = \frac{\partial f}{\partial z}(z(t, q_0); q_0)$$

and

$$g_0 = \frac{\partial f}{\partial q}(z(t, q_0); q_0).$$

The solution to this system of ODEs yields the local system sensitivity about the point $\mathbf{q_0} \in Q_{ad}$ which we will use to examine the sensitivity of the states with respect to the parameters over time.

3.2 Forward Solution of the ODE

Note that the solution of the matrix system of ODEs depends on having a solution to the original model of ODEs (see equation for $\dot{\mathbf{z}}$ above). Therefore, to employ our sensitivity results, we first must be able to solve the original model. To this end, we employed the MATLAB stiff ODE solver *ode15s*. We used parameters values $\mathbf{q_0}$ as given in the table in Section 2.3 and initial condition $\mathbf{z}_0 = [10, 0.3, 0.008, 0.001, 7.5]$. Solutions were found over different time spans, e.g., 100 days and 500 days.

3.3 Sensitivity of $\frac{\partial J}{\partial \mathbf{q}}(\mathbf{q_0})$ Based on the Cost Function $J(q)$

The cost function,

$$J(\mathbf{q}) = \frac{\sum_i \left|\log(C * \mathbf{z}(t_i, \mathbf{q})) - \log(C * \hat{\mathbf{z_i}})\right|^2}{\sigma_i^2},$$

gives a measure of how well the values predicted by the model for $\mathbf{z}(t_i)$ fit the experimental data $\mathbf{z_i}$. Therefore, analyzing

$$\frac{\partial J}{\partial \mathbf{q}}(\mathbf{q_0}) = \sum_i 2\frac{\log(C * \mathbf{z}(t_i, \mathbf{q_0})) - \log(C * \hat{\mathbf{z_i}})}{\sigma^2 \cdot (C * \mathbf{z}(t_i, \mathbf{q_0}))} \cdot \left(C * \frac{\partial \mathbf{z}}{\partial \mathbf{q}}(t_i, \mathbf{q_0})\right)$$

gives us an idea of how sensitive this fit is to small changes in any one of the parameters. Since we did not have experimental data with which to work, we instead used the solution to the original system of ODEs found using the MATLAB stiff solver $ode15s$ and added random noise to it in the following manner:

$$\log \hat{\mathbf{z}}_\mathbf{i} = \log \mathbf{z}(\mathbf{t_i}) + \eta\epsilon(t_i),$$

where $\hat{\mathbf{z}}_\mathbf{i}$ = simulated data at time t_i, η = error range percentage, and $\epsilon(t_i)$ is randomly distributed according to an N(0,1) normal distribution.

Figure 3 depicts the values we obtained for $\log|\partial J/\partial \mathbf{q}|$ over 100 different simulated data sets. This particular plot represents results for the system with no treatment (i.e., $u = 0$). We also carried out the same analysis for the system under the periodic treatment interruption mentioned earlier in the paper and found the the same four parameters β, a, p, c were still the most sensitive and that the drug efficacy f became the fifth most sensitive parameter.

Throughout the paper, the boxplot of a data set is a box and whisker plot where the box has lines at the lower quartile, median, and upper quartile values. The whiskers are lines extending from each end of the box to show the extent of the rest of the data. The whiskers end at the data points that lie just within 1.5 of the interquartile range (IQR). Outliers are data with values beyond the ends of the whiskers.

3.4 Sensitivity of Parameters Over Time

One benefit of the sensitivity matrix,

$$\frac{\partial \mathbf{z}}{\partial \mathbf{q}}(t, \mathbf{q_0}),$$

is that it illustrates the time dependence of the sensitivity of each compartment to each parameter. If we choose a particular parameter, we can plot the sensitivity of each compartment with respect to that parameter as a function of time and use this information to decide when measurements of those compartments will be most beneficial. Since many of the laboratory measurements can be costly, it is important to minimize the number of measurements. For our simulated data, we can construct a data measurement schedule and then interpolate at those time values. Using this data we can then compute the sensitivity of the cost function to our parameters.

For example, in the model with no drug treatment, i.e., $u(t) = 0$, we observed that β (infection rate), c (immune effector activation rate), a (natural death rate of infected cells), and b (natural death rate of the immune effector) are most sensitive. In Figure 5, we observe very different behavior of the sensitivity to each of these parameters as functions of time.

Although these plots only represent the sensitivity of the viral compartment, Figure 6 shows that the sensitivity of the other compartments is qualitatively similar.

The system appears to be most sensitive to β initially, but this reduces quickly and then begins to dominate again as time progresses. Hence, we would suggest measuring $\mathbf{z}$ after five days, waiting a month, and then beginning weekly measurements. Using this measurement scheme, Figure 4 shows an increase in the relative sensitivity to β. Similarly, since sensitivity to a remains high throughout time, we would recommend regular measurement throughout the entire observation period (e.g., weekly). The sensitivity to c is high initially, but then decreases rapidly, so we might recommend measuring every third day for six weeks and then discontinuing

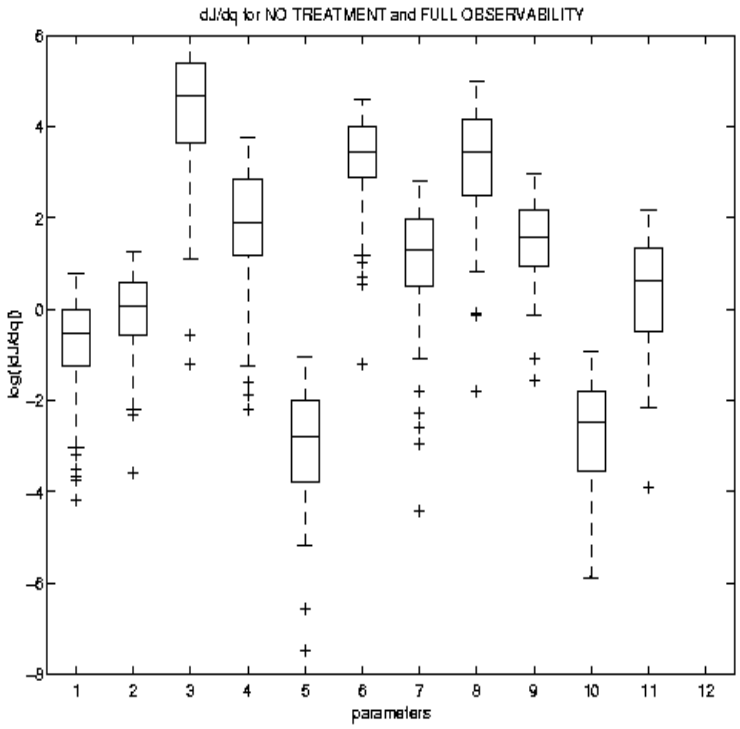

Figure 3: Log scale plot of sensitivity of the cost function to our twelve parameters, where the indices along the x-axis correspond to the parameters in the same order found in Section 2.2. Full observability means $C = I$

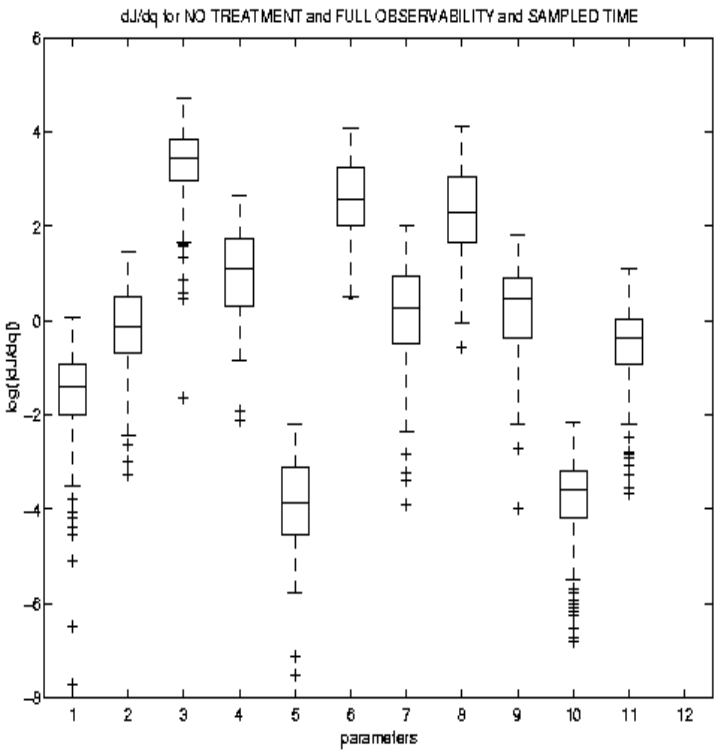

Figure 4: Log scale plot of sensitivity of the cost function to our twelve parameters after implementing a measurement scheme based on the sensitivity of β over time. Again, $C = I$.

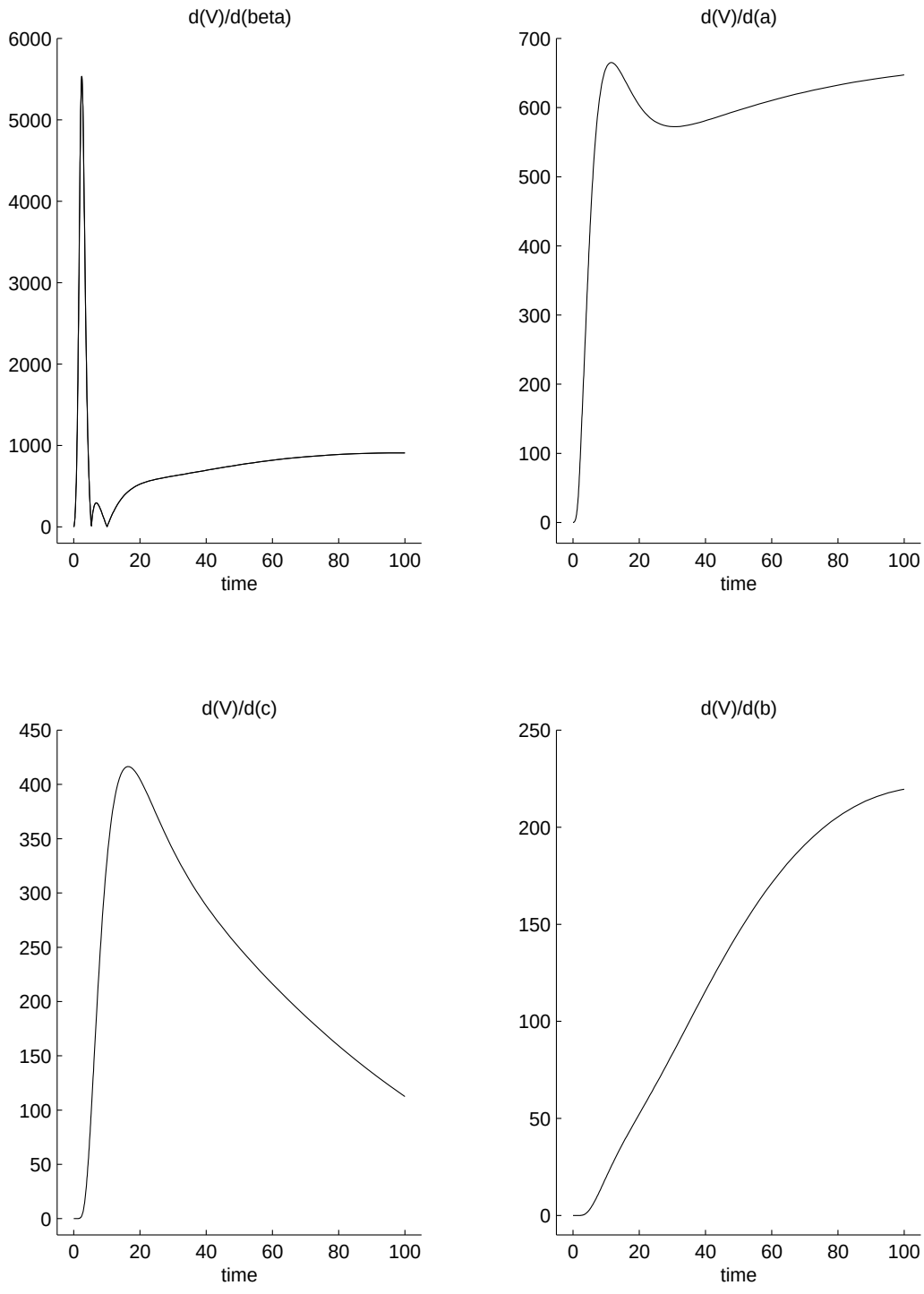

Figure 5: Plots of the sensitivity of the viral load V to parameters β, a, c, and b over 100 days of no treatment.

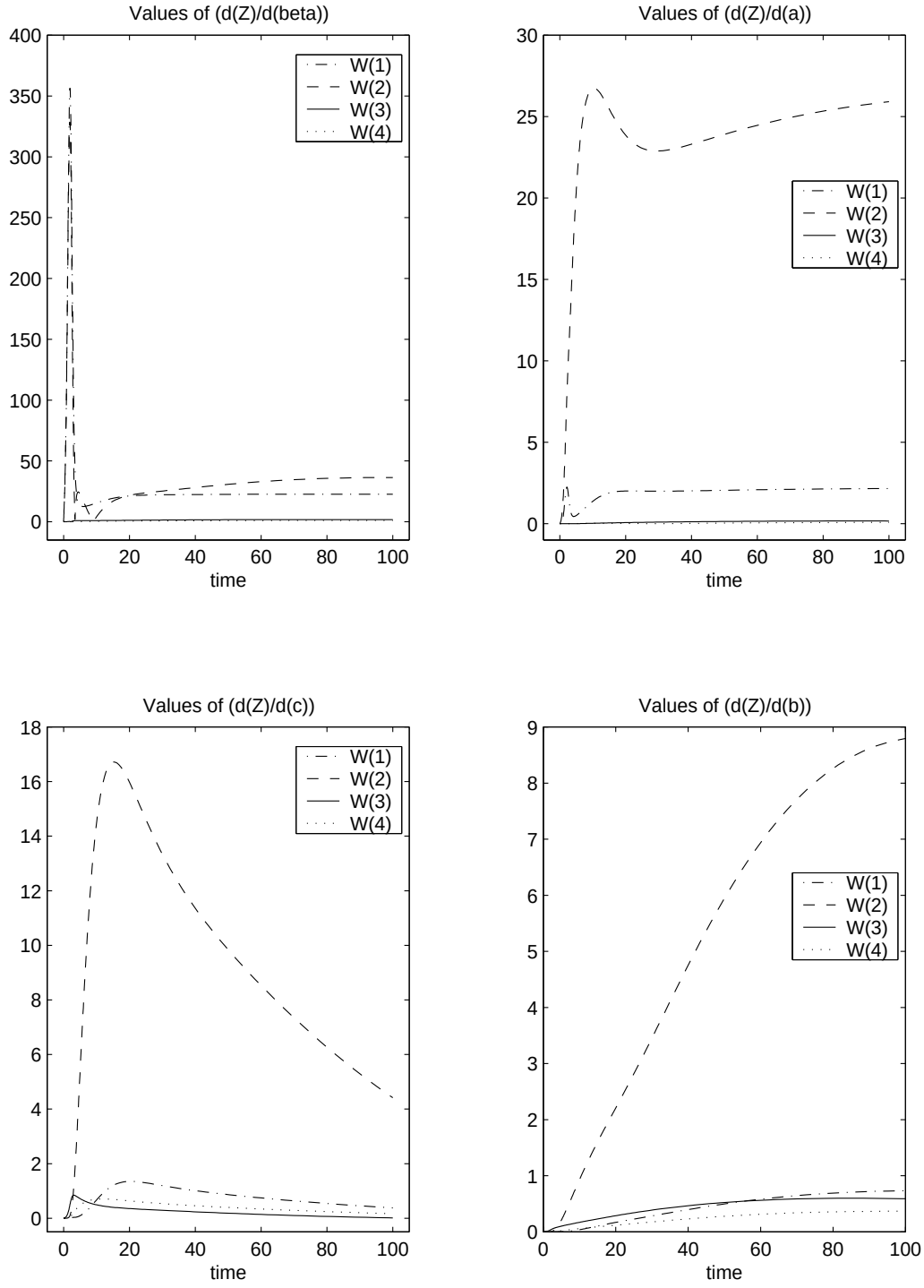

Figure 6: Plots of the sensitivity of the first four compartments, where $Z = W(1)$, etc., to the same four parameters as in Figure 5.

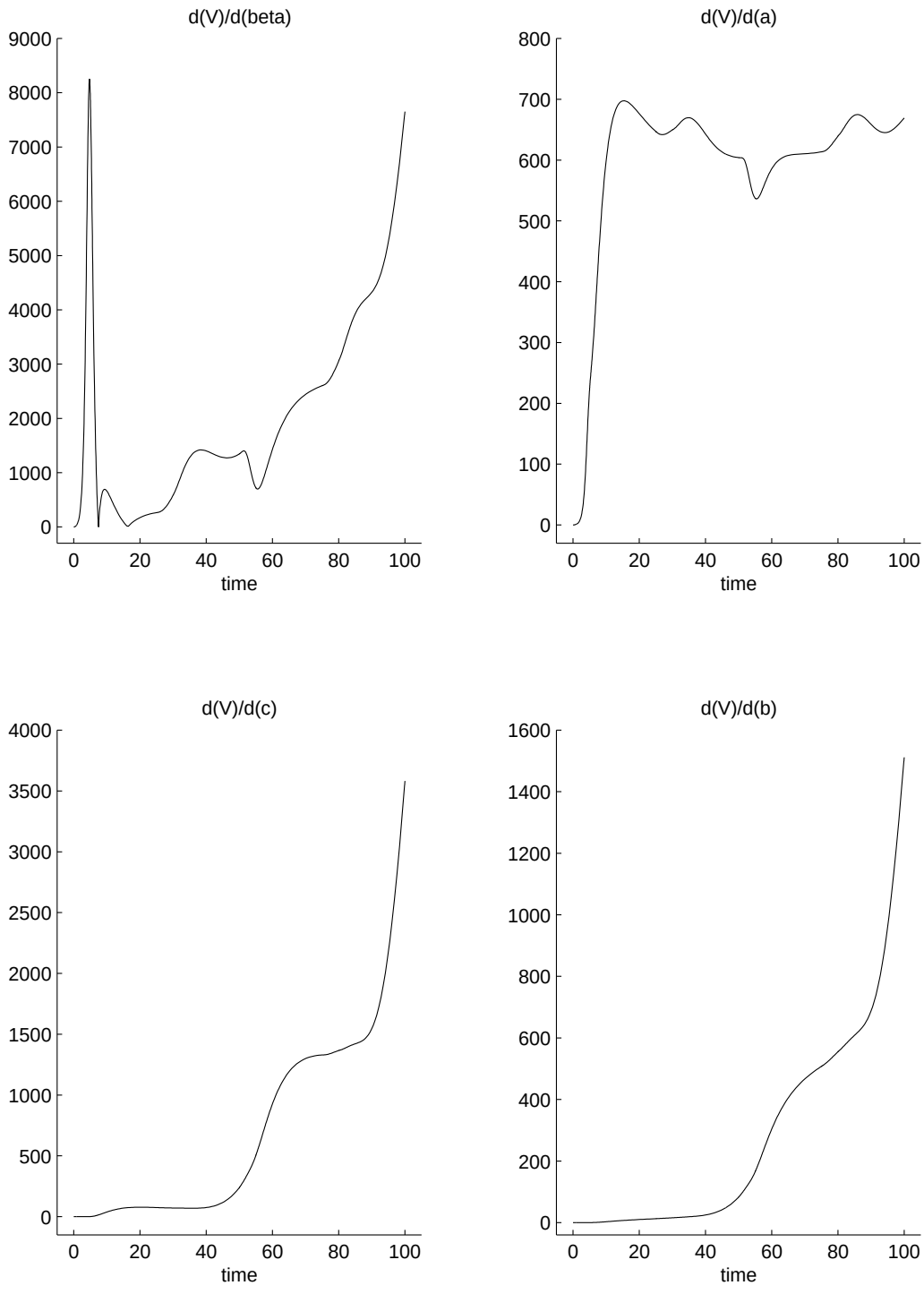

Figure 7: Sensitivity of the viral load over 100 days of periodic STI.

measurements. For b, we might recommend just the opposite approach. As a result, it is difficult to recommend a measurement schedule for estimating all four of our most sensitive parameters. Perhaps the best approach is simply to measure at regular intervals.

When the structured treatment interruption described in Section 2.2 is introduced, the qualitative behavior of the sensitivity matrix changes. As observed in Figure 7, our previous measurement schemes for a and b may still be appropriate, whereas we need to modify those for β and c. Since the sensitivity to β now begins to increase rapidly after two months, we need to measure more frequently instead of on a weekly basis. Similarly, our measurement scheme for c should now mimic the one for b, since the sensitivities to those parameters are very similar.

3.5 Observation Matrices

The cost of data collection varies widely across the five compartments in the model. The viral load V is often the only compartment measured. The uninfected cells X and the infected cells Y, can be measured together with considerably less expense than measuring them separately. The same is true for the immune precursors W and the immune effectors Z. In order to suggest an effective and frugal experimental protocol, it is useful to determine which compartments measurements are essential and whether combining or eliminating compartments compromises the quality of the data. In order to answer these questions, we created a set of observation matrices C_i to represent different combinations of compartments. When our compartmental vector is multiplied by one of these observation matrices, we change the observations made in the parameter estimation problem.

The observations we examined were:

Observations
$[X, Y, W, Z, V]$
$[X, Y, W+Z, V]$
$[X+Y, W+Z, V]$
$[X+Y, W+Z]$
$[X, Y, V]$
$[X+Y, V]$
$[V]$

3.6 The Effect on $\frac{dJ}{dq}$ from Changing the Observables

Our next step was to incorporate different observation matrices C into the cost function and analyze $\frac{dJ}{d\mathbf{q}}$ for each. To summarize the results, measuring only $[V]$, or $[X+Y, V]$ causes a significant loss in sensitivity with respect to most parameters, whereas the results obtained with $[X+Y, W+Z]$, $[X+Y, W+Z, V]$, and $[X, Y, W+Z, V]$ are strikingly similar to those obtained with the full set of observables $[X, Y, W, Z, V]$. As in Section 3.3 we used a time sampling of once a day for 100 days in each data set, and the results below are for the untreated model. Similar results were obtained in the treated model. Figures 8 and 9 illustrate the changes that occur in the sensitivity of our cost function as we change the observation matrix. The 100 different data sets used to generate the results for any one of the observation matrices were not the same as the data sets used for any of the other observation matrices.

4 The Inverse Problem: Estimating the Parameters

4.1 Why solve the Inverse Problem?

All of the analysis in this paper is based on the the modified Wodarz-Nowak Model. Now we concern ourselves with another question: *Is our model a good model?* One way to answer this question is to answer another

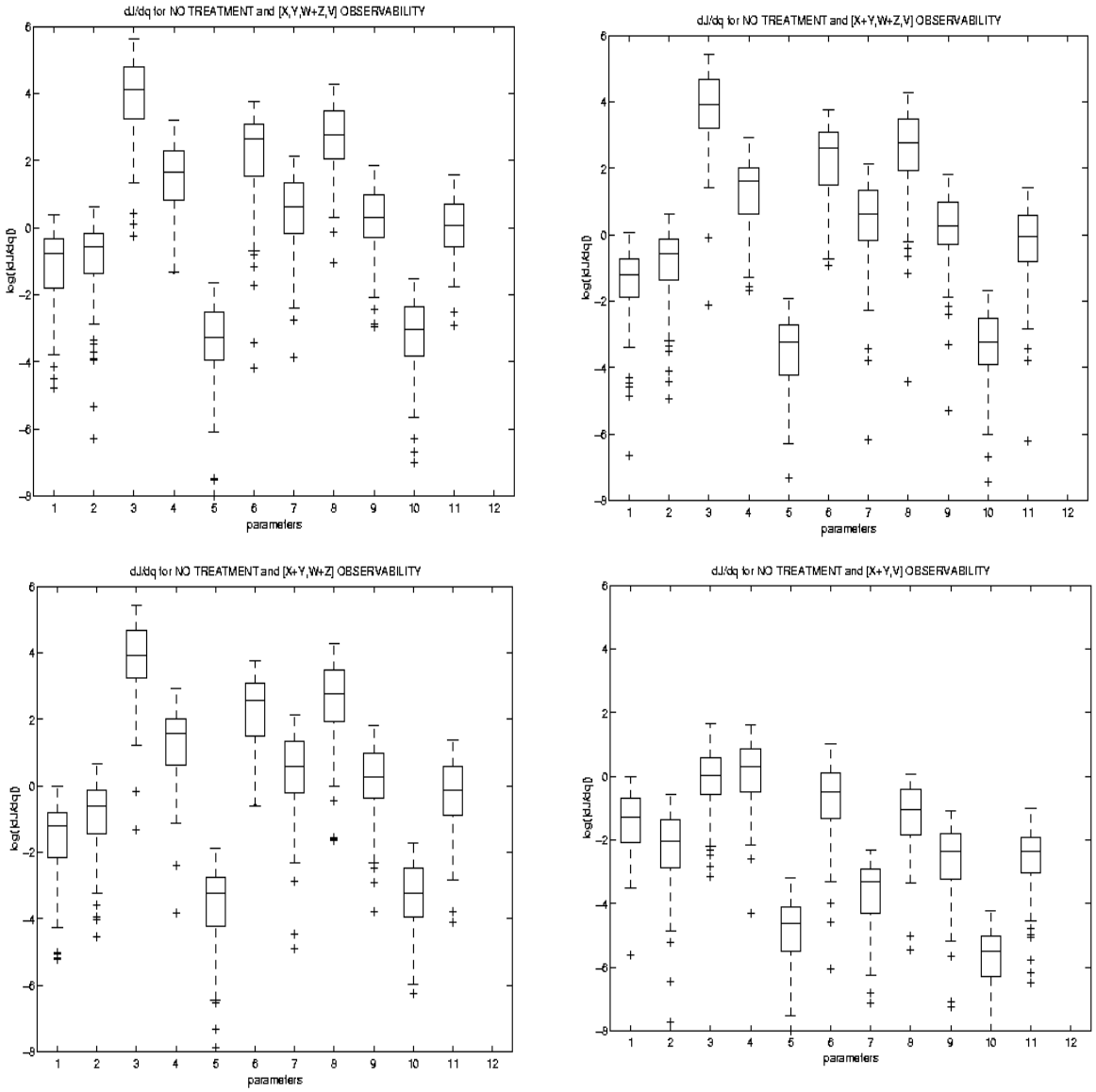

Figure 8: $\frac{dJ}{d\mathbf{q}}$ for various observation matrices.

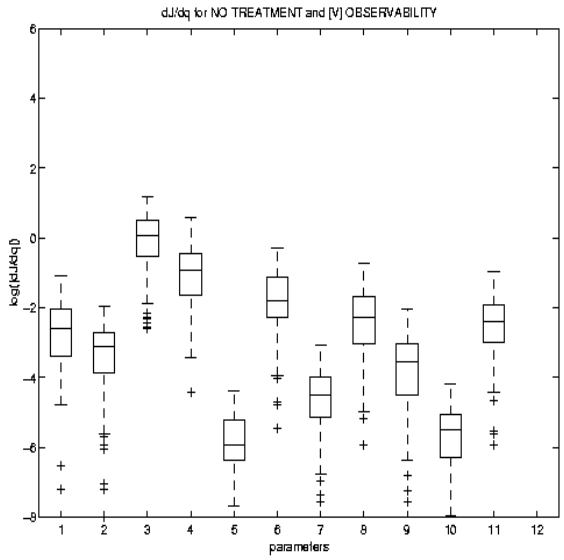

Figure 9: $\frac{dJ}{d\mathbf{q}}$ when only the viral load is observed.

question instead: *Given a data set, does our model describe the data set?* Solving the inverse problem answers the latter question.

Inverse problems arise in a variety of important applications in science and industry. These range from biomedical and geophysical imaging to groundwater flow modeling. In all these applications the goal is to estimate some unknown attributes of interest, given measurements (a data set) which are indirectly related to these attributes. For example, in medical tomography, one wishes to image structures within the body from measurements of X-rays which have passed through the body [9]. For our model, the data set which the immunologist can measure is the vector of observables $\hat{\mathbf{y}} = C\hat{\mathbf{z}}$. For instance, $\hat{\mathbf{y}}$=[X + Y, V] indicates that the data available is the total count of X plus Y, the combined total of uninfected T helper cells and infected T helper cells, and V, the number of free virions. The attributes of interest that we wish to estimate given the data $\hat{\mathbf{y}}$ are the components of $\mathbf{q}$.

Solving the inverse problem identifies the parameters $\mathbf{q}^*$ for which the model best describes the given data $\hat{\mathbf{y}}$. That is, we determine $\mathbf{z}(\mathbf{q}^*)$ so that the "distance" between $C\mathbf{z}(\mathbf{q}^*)$ and $\hat{\mathbf{y}}$ is as small as possible. We use the least squares cost function,

$$J(\mathbf{q}) = \frac{\sum_i |\log(C * \mathbf{z}(t_i, \mathbf{q})) - \log(C * \hat{\mathbf{z}_i})|^2}{\sigma_i^2},$$

to determine this distance. Therefore, solving the inverse problem is equivalent to solving $\mathbf{q}^*$ such that

$$\mathbf{q}^* = \text{argmin}_{\mathbf{q} \in Q_{ad}} J(\mathbf{q}) = \frac{\sum_i |\log(C * \mathbf{z}(t_i, \mathbf{q})) - \log(C * \hat{\mathbf{z}_i})|^2}{\sigma_i^2}$$

where Q_{ad} is called *Q-admissible*, the space of valid values for $\mathbf{q}$.

Given a data set, does our model describe the data set? The answer is yes if $J(\mathbf{q}^*)$ is "small".

4.2 Implementation

4.2.1 Simulating Data

To formulate the inverse problem requires data. Since we did not have access to real data, we simulated data by

$$\log \hat{\mathbf{z}}_\mathbf{i} = \log \mathbf{z}_\mathbf{i} + \sigma\epsilon_i,$$

where $\epsilon_i = \epsilon(t_i) \sim N(0,1)$ and we assumed the vector of measurement errors were $\sigma^2 = [.01.01.01.01.25] \cdot \lambda$, for $\lambda \geq 1$. That is, σ^2 is the error incurred when a clinician actually measures each compartment. Therefore, when we generate data we are assuming that X, Y, W and Z are each measured with 1% error from the true measurement and V is measured with 25% error from the true measurement.

Since we are assuming that X, Y, W, Z, V are mutually independent, then for example we can assume that the measurement error for measuring X and Y together is the sum of the measurement errors of measuring X and then Y individually. Hence, the measurement error for $C\hat{\mathbf{z}}_\mathbf{i}$=[X + Y] is $\sigma_X^2 + \sigma_Y^2$.

4.2.2 Optimization Methods

To find $\mathbf{q}^*$, we used the Nelder Mead simplex method (MATLAB's *fminsearch*). We tried other optimization methods, including Steepest Descent, Newton CG and BFGS methods, but Nelder Mead outperformed these for our data. Nelder Mead has the further advantage that the gradient $\nabla_q J = \partial J/\partial \mathbf{q}$ need not be calculated; the method only requires evaluations of the cost function $J(\mathbf{q})$.

4.2.3 Using the Sensitivity Analysis

If it becomes difficult to find $\mathbf{q}^*$ over all the parameters, then we can concern ourselves with optimizing J just over the parameters to which the model is most sensitive. The five most sensitive parameters for the model with treatment in order of sensitivity, identified by the sensitivity analysis that we performed, are

β = proliferation rate of Infected T helper cells,
c = proliferation rate of Immune Precursors Cytotoxic T Lymphocyte,
b = natural death rate of Immune Precursors Cytotoxic T Lymphocyte,
a = natural death rate of Infected T helper cells, and
f = drug efficacy.

4.2.4 Further Assumptions

We solved the inverse problem for thousands of different synthetic data sets $\hat{\mathbf{z}}$, where the error σ^2 was generated for λ=1, 10, 100, 1000, and 10000; and $\mathbf{z} = \mathbf{z}(t_i, \mathbf{q_{true}})$, with $\mathbf{q_{true}}$ =[1, .1, .02, .2, 1 ,.027, .5, .001, .1, 25, 1, .75]. Note that each $J(\mathbf{q})$ evaluation requires a forward solution of the ODE, as in Section 3.2. For each of these, we assumed that $z_{init} = [10, .3, .008, .001, 7, .5]$.

Furthermore, we let C be the identity matrix (so we are assuming *full observability*, that each compartment of $\mathbf{z}$ can be measured), that $t_i = 1, 2, 3, 4, ..., 100$ (measurements for each compartment are taken each day over a 100 days), and that the periodic treatment $u(t)$ is being applied.

4.3 Results

Two general approaches were used. First, for $\mathbf{q_{init}} = \mathbf{q_{gen}}$, synthetic data was generated for λ=1, 10, 100, 1000, and 10000. When the parameters are independent, this approach allows us to estimate a probability density for each of the components of $\mathbf{q}$.

Secondly, we solved the inverse problem for many different values of $\mathbf{q_{init}} = \mathbf{q_{true}} + \mathbf{q_{true}} \cdot \eta\delta$, where $\delta \sim N(0,1)$. As η increases, $\mathbf{q_{init}}$ is perturbed further from $\mathbf{q_{true}}$. Since $\mathbf{q}^* \approx \mathbf{q_{true}}$, this methodology should enable us to estimate a confidence neighborhood about $\mathbf{q_{true}}$ so that for any $\mathbf{q_{init}}$ in this neighborhood we can make a confidence statement about how well our inverse problem algorithm can find $\mathbf{q}^*$ adequately close to $\mathbf{q_{true}}$.

4.3.1 Estimating Probability Densities

As mentioned before, we simulated data by

$$\log \hat{\mathbf{z}}_\mathbf{i} = \log \mathbf{z}_\mathbf{i} + \sigma \cdot \epsilon,$$

where

$$\epsilon \sim N(0, 1),$$

and we assumed the vector of measurement errors was $\sigma^\mathbf{2}$=[.01, .01, .01, .01, .25]$\cdot\lambda$, for $\lambda \geq 1$ where lambda is a scalar to amplify the noise in the data. Simulations were run for lambda=1, 10, 100, 1000 and 10000.

Keeping $\mathbf{q_{init}} = \mathbf{q_{true}}$ fixed, we varied the amount of noise in the data by generating 100 different synthetic data sets for each of the values λ=1, 10, 100, 1000 and 10000. When the parameters are independent, this approach allowed us to construct a marginal probability density for each of the components of $\mathbf{q}$.

Figure 10(a) shows the results of our algorithm for the five most sensitive parameters: β, c, b, a, and f when $\lambda = 10$. Figure 10(b) shows a probability density for β when $\lambda = 10$.

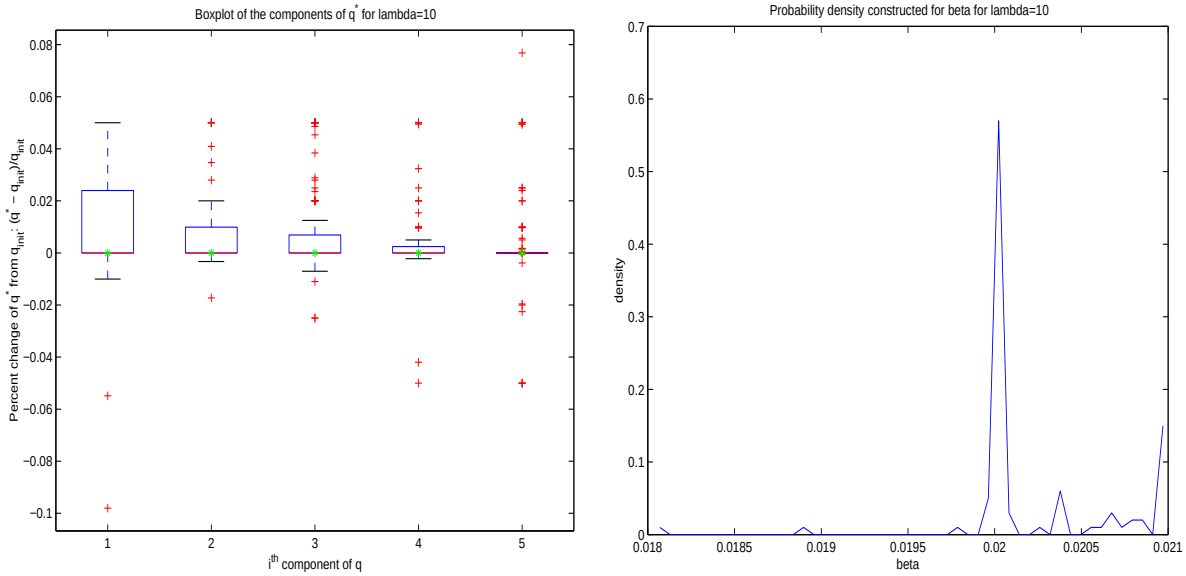

Figure 10: (a) Boxplot of $\mathbf{q}$=[β c b a f] vs the percent variation of each these parameters ($\mathbf{q}^*$) from $\mathbf{q_{true}}$, $\frac{\mathbf{q}^*-\mathbf{q_{true}}}{\mathbf{q_{true}}}$, over 100 inverse problem solves for λ =10. (b) The probability density of beta that we constructed using the results from (a).

4.3.2 Trying to Find a Confidence Neighborhood

First, we attempted to find $\mathbf{q}^*$ over all twelve parameters. For η =.01, .05, and .1, we saw that the $\mathbf{q}^*$ procured from our algorithm was not very far from $\mathbf{q_{init}}$ (see Figure 11). For values of $\eta \geq .2$ (for large perturbations of $\mathbf{q_{init}}$ from $\mathbf{q_{true}}$, the Nelder Mead algorithm was unable to solve the system at all. Hence, we turned to the results of our sensitivity analysis to make the optimization problem simpler.

As mentioned earlier, when it becomes difficult to find $\mathbf{q}^*$ over all the parameters, then we can concern ourselves with optimizing J just over the parameters to which the model is most sensitive. Therefore, we set $\mathbf{q_{true}}$ =[β c b a f], the five most sensitive parameters.

The only benefit to this approach was that we were able to solve the system for $\eta \leq .5$. Unfortunately, the $\mathbf{q}^*$ procured from our algorithm still was not very far from $\mathbf{q_{init}}$, as seen in Figure 12. Hence a new optimization scheme is recommended which is not so dependent on $\mathbf{q_{init}}$.

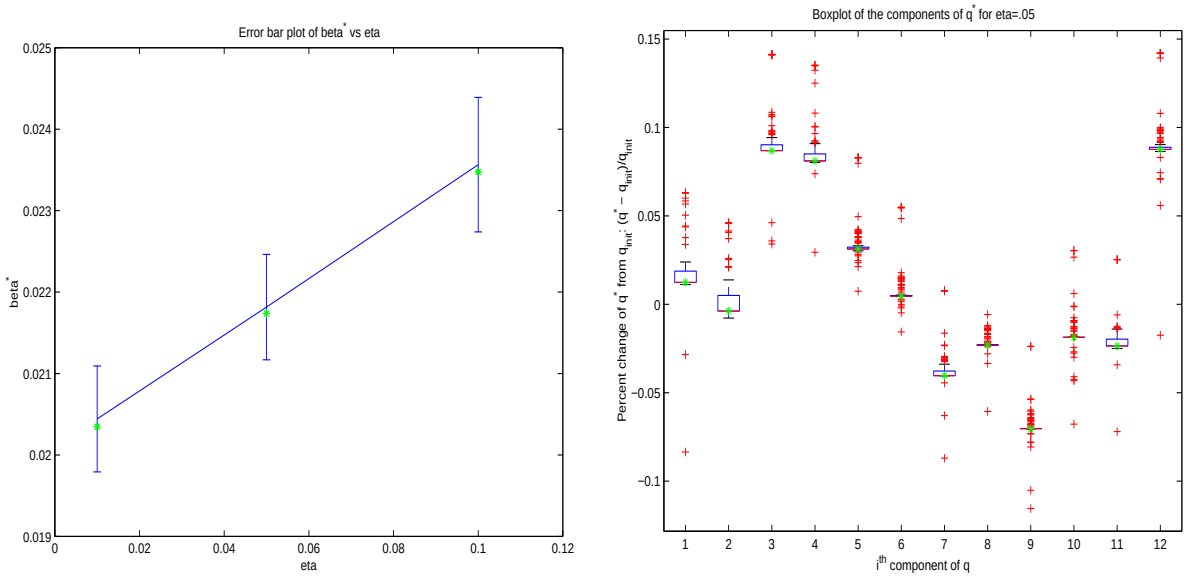

Figure 11: (a) When optimizing over all the parameters, this is the error plot of optimal β, β^*, vs η, the perturbation applied to β_{true} to generate β_{init}. The value of β_{init} is indicated by an '*'. For the same $\mathbf{q_{init}}$, the inverse problem was solved 100 times, with a different synthetic data set for each solve, for η: η =.01, .05, and .1. Since $\mathbf{q_{init}} = \mathbf{q_{true}} + \mathbf{q_{true}} \cdot \eta N(0,1)$ then, for each η, $\beta_{init} = .02 + .02 \cdot \eta N(0,1)$. Error bars indicate 2 standard deviations about the mean for the 100 different inverse problem solves. β^* is directly related to the perturbation of β_{init}. In fact, for for $\eta \geq .05$, $\beta^* > .15\beta_{true}$. (b) When optimizing over all parameters, this is the boxplot of the components of $\mathbf{q}$ vs the percent variation of each component of $\mathbf{q}^*$ from $\mathbf{q_{true}}$, $\frac{q^* - \mathbf{q_{true}}}{\mathbf{q_{true}}}$, over 100 inverse problem solves for η =.05. $\beta = \mathbf{q}[3]$. These plots indicate that we ought to try constraining our optimization to the parameters that affect the model the most.

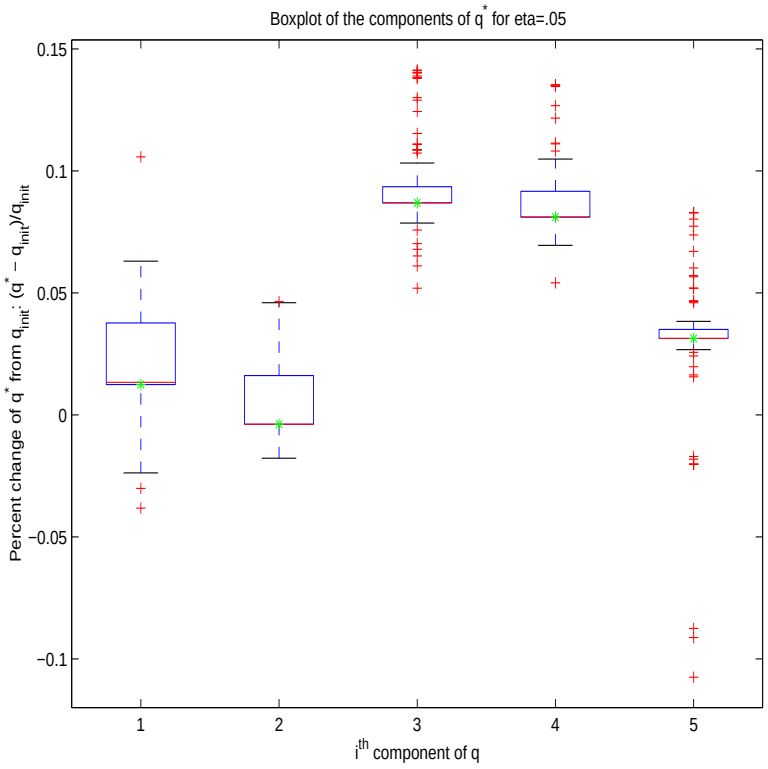

Figure 12: When optimizing over the 5 parameters which affect the model the most, $\mathbf{q}$=[β c b a f], this is the boxplot of the components of $\mathbf{q}$ vs the percent variation of each component of $\mathbf{q}^*$ from $\mathbf{q_{true}}$, $\frac{\mathbf{q^*-q_{true}}}{\mathbf{q_{true}}}$, over 100 inverse problem solved when η =.05. These plots indicate that even when constraining our optimization to the parameters that affect the model the most, $\mathbf{q}^*$ is still far from $\mathbf{q_{true}}$. Hence a new optimization scheme is recommended which is not so dependent on $\mathbf{q_{init}}$.

5 Conclusion

The results of our investigations provide some guidance for future study, including design of experiments aimed to investigate the efficacy of STIs, the validity of the modified Wodarz-Nowak model for HIV infection dynamics, and estimates for the parameters in the model.

Our first set of results from the sensitivity analysis concerns the parameters in the model. The sensitivity analysis determined that the parameters β, a, p, c were still the most sensitive and that with treatment, the drug efficacy f becomes the fifth most sensitive parameter. These parameters play significant roles in the dynamics of the model.

Our second set of results from the sensitivity analysis suggests times to collect data about the parameters. Without STI, the system is most sensitive to β initially, which reduces quickly and then begins to dominate again as time progresses. We suggest measuring $\mathbf{z}$ after five days, waiting a month, and then beginning weekly measurements. Since sensitivity to a remains high throughout time, we would recommend regular measurement throughout the entire observation period (e.g., weekly). The sensitivity to c is high initially, but then decreases rapidly, so we might recommend measuring every third day for six weeks and then discontinuing measurements. For b, we recommend the opposite approach. Because the results for each parameter suggest a different measurement schedule, we suggest that the best approach may be to measure at regular intervals. With STI, the sensitivity to β now begins to increase rapidly after two months. Consequently, with the introduction of STI, we suggest more frequent measurement.

Our third set of results from the sensitivity analysis indicates which combinations of compartments play a significant role in the dynamics of the model. Measuring only $[V]$, or $[X + Y, V]$ causes a significant loss in sensitivity with respect to most parameters, whereas the results obtained with $[X+Y, W+Z]$, $[X+Y, W+Z, V]$, and $[X, Y, W + Z, V]$ are strikingly similar to those obtained with the full set of observables $[X, Y, W, Z, V]$. This is a very useful result, since combining measurement of X with Y and W with Z leads to a large reduction in cost of data collection without sacrificing the quality of the information collected.

In our work with the inverse problem, we have discovered the probability distributions for optimal β, c, b, a, and f the parameters to which the model is most sensitive, given the synthetic data sets that we constructed. Although our approach was not able to achieve a solution for the inverse problem over all twelve parameters, limiting the optimization to the most sensitive parameters results in some increase in the ability of the optmizer to converge to the optimal parameter set.

Some questions for future consideration concern the details of the experimental protocol and future attempts to solve the inverse problem. One issue of particular concern is how to time the STIs given that a "day" in our model may not correspond to real time. Once data have been collected, the inverse problem can be reexamined to find better estimates for parameters in the model.

6 Acknowledgements

The authors would like to thank Dr. Sarah Holte of the Fred Hutchinson Cancer Research Center as well as Dr. H. T. Banks, Brian Adams and David Bortz of North Carolina State University for their guidance and assistance.

References

[1] Lisziewicz J, Rosenberg E, Liebermann J et al., "Control of HIV despite the discontinuation of antiretroviral therapy." *New England Journal of Medicine* 340:1683-4, 1999.

[2] Rosenberg, E. S., M. Altfeld, S. H. Poon et al. *Nature* 407:523-526, 2000.

[3] Wodarz, D., and M.A. Nowak, "Specific therapy regimes could lead to long-term immunological control of HIV." *Proc Natl Acad Sci USA* 96, 14464-9, 1999.

[4] Coddington, Earl A., and Levinson, Norman, Theory of Ordinary Differential Equations, McGraw-Hill, New York, 1955.

[5] Bonhoeffer, S., M. Rembiszewski, G. M. Ortiz, and D. F. Nixon, "Risks and benefits of structured antiretroviral drug therapy interruptions in HIV-1 infection." *AIDS* 14:2313-2322, 2000.

[6] Davey RT. N. Bhat, C. Yoder et.al. 1999. *Proc. Natl. Acad. Sci* 96:15109-14.

[7] Garcia, F., M. Plana, C. Vidal et al. *AIDS* 13:F79-F86.

[8] Ortiz G, Nixon D, Trkola A et al., "HIV-1-specific immune responses in subjects who temporarily contain antiretroviral therapy." *J Clin Invest* 104:R13-R18, 1999.

[9] C.R. Vogel, "Computational Methods for Inverse Problems", preliminary manuscript, to be published by SIAM, available on the web at www.math.montana.edu/∼vogel/Book